

ac susceptibility of the ferromagnetic phase of the *AuFe* system

I. Maartense and Gwyn Williams*

Department of Physics, University of Manitoba, Winnipeg, R3T 2N2, Canada

(Received 29 November 1976)

The ac susceptibility of a Au-22-at.-%-Fe alloy has been studied as a function of both applied field and thermal history in the vicinity of the Curie temperature T_C . The principal maximum in the ac susceptibility becomes weaker, broader, and moves to lower temperatures relative to the zero-field maximum, as the external field is increased. A second narrower peak is consequently observable, and is identified as the true critical peak. Analysis of the critical behavior reveals that the exponent $\gamma = 1.51$ while $\delta = 3.6$ for the as quenched sample, and its effective Fe moment is estimated at about $6\mu_B$. The effects of thermal history are striking; T_C is found to increase from 213 to 278°K on aging the rapidly quenched specimen for 1500 h at 24°C, but subsequent aging between 100 and 300°C causes T_C to fall to about 228°K. Both γ and μ_{eff} are unchanged by such treatment, but the apparent value for δ increases to 3.9. These results are *not* consistent with the formation of large magnetic clusters (or precipitates) during heat treatment, but may be explained by the occurrence of short-range order which varies the arrangement of magnetic neighbors.

I. INTRODUCTION

The *AuFe* system is perhaps the most extensively examined alloy system, having recently been subjected to study by small-angle critical neutron scattering,¹ asymmetric positron emission from positive muon decay,² and ac susceptibility measurements³ as well as by electrical,⁴ thermoelectric,³ thermal,⁵ Mössbauer,⁶⁻¹⁰ and magnetic techniques.¹⁰⁻¹⁴ The consensus emerging from the analysis of these data indicates that below 25-ppm Fe it acts as an essentially isolated impurity system with a Kondo temperature of about 0.24°K. Above this concentration interimpurity interactions are observed, which result in the occurrence of magnetic ordering of various types. In the concentration range 0.5- to 8-at.-% Fe these alloys are considered to be spin glasses, with the paramagnetic to spin-glass transition being characterized by a sharp cusp in the zero-field ac susceptibility³ $\chi_0(T)$ at the spin-glass ordering temperature. The mictomagnetic regime occurs above 10-at.-% Fe, where large Fe clusters and behavior strongly dependent on thermal history are observed (ordering temperatures can reportedly^{14,15} be changed by up to 50°K by varying heat treatments), while it has also been suggested^{14,16} that large-cluster superparamagnetism occurs in this region. Finally, for Fe concentration in excess of 17 at.-%, long-range ferromagnetism occurs. Even for these higher concentrations, thermal history effects have been reported.¹⁷

In this paper we report measurements of the ac susceptibility $\chi(T)$ of Au-22-at.-% Fe, an alloy whose concentration is well into the region of long-range ferromagnetic order. We have previously reported the ac susceptibility of the ferromagnetic

exchange-enhanced systems¹⁸ *PdCo* and¹⁹ ($\text{Pd}_{95}\text{Rh}_5$)Co and presented evidence that in such systems the principal maximum in $\chi_0(T)$ did *not* coincide with the ferromagnetic ordering temperature T_C , in contrast to the behavior reported³ for spin glasses. In these dilute ferromagnetic alloys it was demonstrated that the principal maximum in $\chi(T)$ became weaker, broader and moved to lower temperatures relative to the zero-field maximum as the dc biasing field was increased; this weakening, however, allowed a second narrower peak to be observed which exhibited a small upward shift in temperature with increasing applied field. For the *PdCo* system it was argued that this behavior (as a function of field) provides strong evidence that the secondary and not the principal maximum in $\chi(T)$ is the true critical susceptibility maximum resulting from a divergence in the susceptibility at the onset of long-range magnetic order; supplementary evidence supporting this assignment came from the analysis of the ($\text{Pd}_{95}\text{Rh}_5$)Co data where it was shown that the ordering temperature T_C derived from the position of the secondary peaks agreed within experimental error with those derived from a resistivity study²⁰ on the same set of alloys, whereas those derived from the principal maxima certainly did not.

The data on the *AuFe* system reported in this paper display many of the characteristics discussed above and previously reported for the *PdCo* and ($\text{Pd}_{95}\text{Rh}_5$)Co systems; in addition we present two new features: (i) an analysis of the critical isotherm $[\chi(H)]_{T_C}$ and the zero-field susceptibility immediately above T_C which, for various reasons, were not examined in the two systems mentioned above. (ii) a direct measurement of the Curie temperature, as it depends on thermal history; we

find that even with 22-at.% Fe there remains a behavior normally associated with the mictomagnetic regime.

II. EXPERIMENTAL DETAILS

The starting materials used in the alloy preparation were 99.999%-pure Au splatters (from Atomergic Chemetals, New York) and 99.999%-pure Fe powder (from Johnson Matthey, London). The Au was first melted on the water-cooled Cu hearth of an argon-arc furnace using a tungsten electrode, to form a button with an approximate mass of 2 g. The button was cold rolled into sheet form, in which the appropriate amount of Fe powder was subsequently wrapped, and then returned to the arc furnace. The alloy was removed from the arc furnace after the first melt and reweighed; the melting losses were negligibly small. The alloy was then replaced in the furnace and homogenized by inverting and remelting it six times.

As there exist many reports in the literature pertaining to thermally induced changes^{4,14,15,17} in the magnetic properties of the AuFe system, we attempted to quench the sample in the shortest time possible. Consequently, the alloy was cold rolled into a sheet of thickness $\sim 40 \mu\text{m}$. A section of this sheet weighing $\sim 0.2 \text{ g}$ was sealed in Vycor tubing and annealed for 3 days at 920°C in a vacuum of 10^{-6} Torr; it was then quickly plunged into iced water, the Vycor tubing being smashed immediately on entering the water bath. After a thin sliver was cut from it, the AuFe sample was mounted in a previously described¹⁹ ac susceptibility apparatus that had been precooled to liquid-nitrogen temperature. We estimate the total time the sample spent at room temperature to be 3 min.

While the procedure described above, combined with the sheet form of the specimen, produced more effective quenching of the entire volume of the sample compared with, say, a spherically shaped sample of comparable mass (lower surface to volume ratio), it did preclude an accurate evaluation of the specimen's demagnetizing factor.

The composition of the sample was checked for us by Dr. P. Gaunt of this laboratory, who performed x-ray diffraction measurements on the aforementioned sliver. These revealed a lattice constant of 4.0172 \AA which, compared with the data of Jette *et al.*,²¹ indicated a composition of 21.7-at.% Fe.

III. RESULTS AND DISCUSSION

The ac susceptibility data reported below were obtained at 5 kHz in an ac driving field of 0.6-Oe rms. The somewhat irregular sample shape pre-

vented accurate corrections for demagnetizing effects, although we estimate the sample's average demagnetizing factor to be close to 0.5. Both the $\chi(T)$ recordings and the internal fields subsequently used in the various critical plots were corrected using this value for the demagnetizing factor. We have attempted to obtain absolute susceptibility values by calibrating the system with a MnF_2 sample having approximately the same filling factor as the AuFe specimen. While relative susceptibility values can be determined with high precision, the absolute values are uncertain to typically $\pm 10\%$. In order to optimize various features (such as those in Fig. 1) it was not always convenient to operate the magnetometer in a calibrated mode; under these circumstances relative susceptibility values only are reported.

A. Behavior in the vicinity of T_C

In Fig. 1 we show the ac susceptibility $\chi(T)$ of the quenched sample as a function of temperature in zero field and in parallel dc applied fields of 10, 25, 50, and 75 Oe. The purpose of this figure is twofold: (a) It shows the *depression* of the principal maximum in $\chi(T)$ by small applied fields in what is a well established long range ferromagnet; for the alloy investigated here this downward shift of the principal maximum amounts to some 45°K in an applied field of 25 Oe. (b) In addition to this downward shift, the associated weakening and

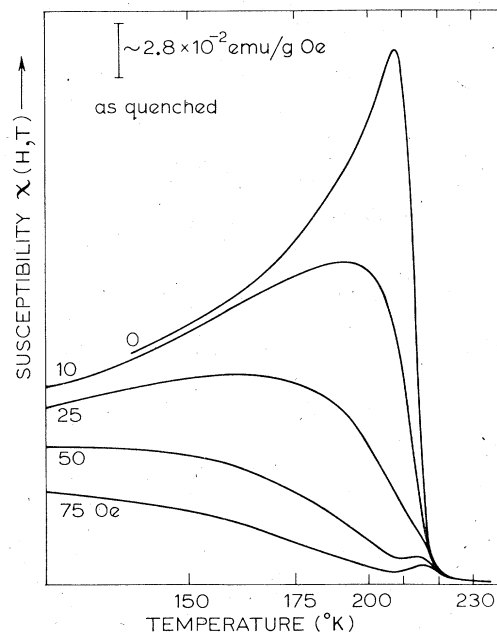


FIG. 1. Measured ac susceptibility of the rapidly quenched Au-22 at.% Fe specimen as a function of temperature in zero applied field, and in dc fields of 10, 25, 50, and 75 Oe.

broadening of the principal maximum allows a second narrower peak to be observed.

Whereas both effects have been reported previously^{18,19} for ferromagnetic alloys, the influence of an applied field with respect to both (a) and (b) is far more striking in AuFe than in any other alloy system we have studied. This point is emphasized in Fig. 2 in which the field dependence of the *second* peak is examined in detail; the ease with which an applied field suppresses the principal maximum and hence allows a study of this second peak is evident from such a figure, which also indicates an *upward* shift in temperature of this latter peak in increasing applied fields. As argued previously^{18,19} the behavior of the principal and secondary maxima as a function of applied field is convincing evidence that the latter and not the former is the true critical peak.

It is possible to obtain $\chi(H)_{T_C}$ from the secondary peaks, and thence to deduce the exponent δ of the critical isotherm²² $M(H)_{T_C} \propto H^{1/\delta}$. From a measured power-law dependence

$$\chi(H)_{T_C} \propto H^{-n}, \quad (1)$$

the critical exponent δ is given by

$$\delta = 1/(1 - n). \quad (2)$$

In Fig. 3(a) we have plotted $\chi(H)_{T_C}$, defined by the height of the peaks, against the internal field H_{int} . The demagnetizing correction was first applied to the measured susceptibility values, whereupon an initial estimate of δ was made. Using this δ , an $M(H)_{T_C}$ plot was constructed to obtain a correction to the applied field, giving the internal field. Due to the non-uniform demagnetizing factor, this procedure is rather dubious at low fields; therefore

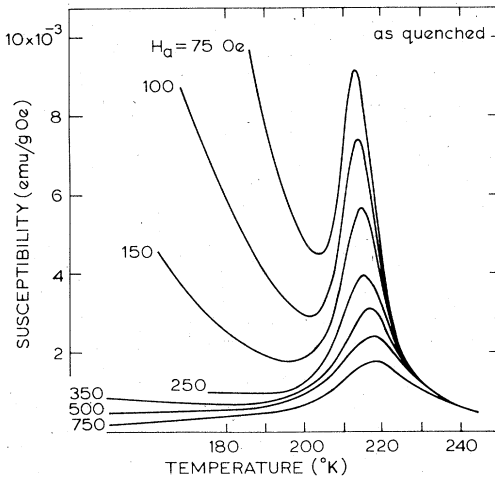


FIG. 2. Detailed analysis of the ac susceptibility (in emu/g Oe) of the secondary peak in various applied dc fields (H_a , in Oe).

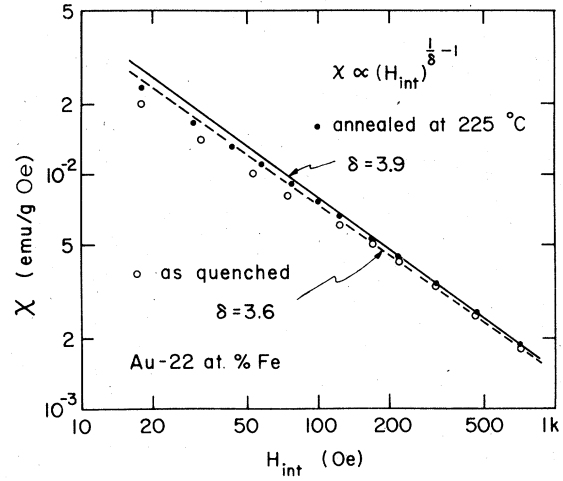


FIG. 3. Log-log plot of the susceptibility at the critical peak, against the internal field H_{int} as defined in the text. (a) The lower data refer to the rapidly quenched sample and (b) the upper points after annealing at 225°C.

only the high-field slope was considered, which then yielded an exponent $n = 0.72 \pm 0.02$, from which we obtain $\delta = 3.6 \pm 0.3$.

This value is somewhat smaller than what is found in elemental ferromagnets (cf.²³ $\delta = 4.2$ in Ni and²⁴ $\delta = 4.35$ in Fe), but this is largely due to a broadening of the critical region in the alloy, as will be discussed below. Nevertheless, this result provides further support for the choice of the secondary maxima as the true critical peaks.

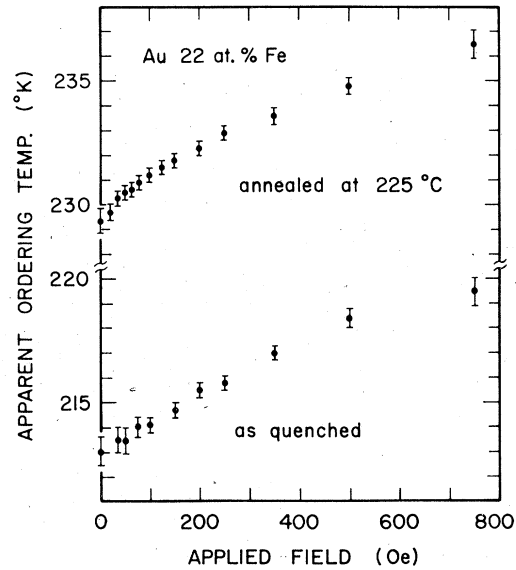


FIG. 4. Field dependence of the position of the critical peak in $\chi(T)$; the zero-field values are the inflexion points in $\chi_0(T)$. The lower plot was obtained from the data represented in Figs. 1 and 2, while the upper plot is derived from the data in Fig. 9.

The ordering temperature, as defined by the position of the critical peaks, is plotted in Fig. 4 as a function applied field. The error bars arise from several sources; at low fields they are primarily due to the rapidly varying background from the nearby principal maximum. At higher fields, where the principal maximum is well removed, the second peak is itself rather broad. Figure 4 shows that the apparent ordering temperature increases with field, and may be extrapolated to render a Curie temperature $T_C = 213.1 \pm 0.5^\circ\text{K}$ in zero field. Within experimental uncertainty this temperature coincides with that of the inflection point of the $\chi_0(T)$ curve, as it does for other systems.^{18,19}

The zero-field susceptibility above T_C can be analyzed to extract the critical exponent γ of the expected power-law dependence²²

$$\chi_0(T) = A\epsilon^{-\gamma}, \quad \text{with } \epsilon = T/T_C - 1. \quad (3)$$

Values of $\chi_0(T)$ taken from the recorded curve were corrected for demagnetization and placed on a log-log plot against ϵ , using the above estimate of T_C . An upward adjustment of 0.4°K from this value was required to obtain a best fit of the data to a straight line for $\epsilon < 3 \times 10^{-2}$. The corrections to χ_0 and T_C had a negligible effect on the slope of $\chi_0(\epsilon)$ for $\epsilon > 5 \times 10^{-2}$, the data are presented in the upper part of Fig. 5.

It is found that $\gamma = 1.51 \pm 0.02$ in the range $2 \times 10^{-2} < \epsilon < 3 \times 10^{-1}$. This value is higher than $\gamma \approx 1.33$, which is commonly quoted for three-dimensional Heisenberg ferromagnets.^{23,24} The critical ampli-

tude A derived from Fig. 5 will be discussed in Sec. III B.

We must consider two factors which might influence the validity of these measured exponents. The first is the spread in ordering temperatures to be expected within a random alloy. The resulting smearing out of the critical region will have a minor effect on the apparent value of γ , and then only close to T_C , and is thus of little concern here where the spreading of the critical region is estimated to amount to no more than 1 or 2°K , or $\Delta\epsilon \leq 10^{-2}$. However the effect of a smeared critical region is extremely important in the case of the critical isotherm. The field dependence of $\chi(H)_T$ drops rapidly on either side of the maximum defining T_C this behavior being strongest at low fields (see Fig. 2). The direct consequence of a broadened critical region is thus a decrease in the measured value of δ as well as a reduction of the critical amplitude. These effects are clearly seen in the experimental results reported in Sec. IV.

The second point to consider is the presence of a small background susceptibility which may arise from magnetic entities such as clusters or paramagnetic regions not taking part in the long-range ordering at T_C (we can safely neglect diamagnetic and similar contributions because of the relatively large values of χ encountered here). The major effect of such entities would be to induce a non-linearity in the plot of $\chi_0(\epsilon)$ (Fig. 5) for $\epsilon > 5 \times 10^{-2}$; no such nonlinearity is observed and hence we conclude that the amount of magnetic precipitates or superparamagnetic clusters present in our sample above T_C is negligibly small. Further confirmation of this conclusion comes from the lack of any observable field dependence in $\chi(T)$ at higher temperatures ($\epsilon > 10^{-1}$). This latter fact is also relevant to the interpretation of changes induced by metallurgical treatment described in Sec. III B.

Finally it should be pointed out that we omit any discussion of possible effects of the thinness of the foil sample on the critical behavior since the present critical analysis is considered to be an investigative tool rather than an end in itself.

B. Effects of heat treatment

All the data discussed above were obtained on a rapidly quenched specimen which had spent about 3 min at room temperature. At no time during the measurements was it allowed to warm to room temperature, and it was stored in liquid nitrogen in intervening times. We emphasize this point because the sample subsequently showed striking effects after aging at room temperature (24°C). Figure 6 details these aging effects; we have

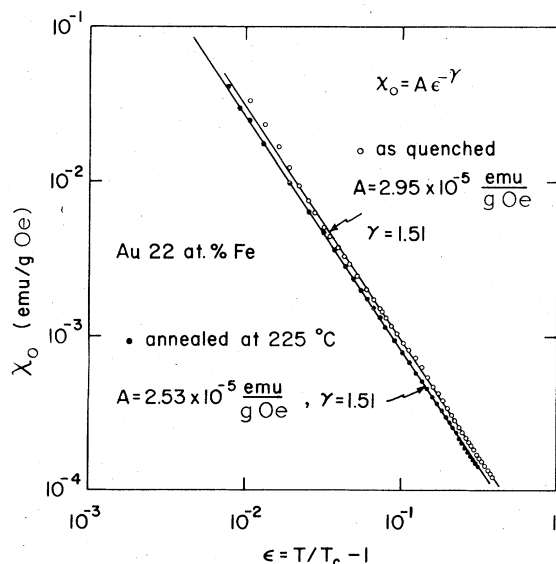


FIG. 5. Critical plots of $\chi_0(T)$ for (a) the rapidly quenched sample and (b) after annealing at 225°C for 15 h.

drawn the ac susceptibility $\chi(T)$, recorded during warming in an applied field of 100 Oe, for a range of aging times. The nonlinear temperature scale in Fig. 6 is a consequence of using the thermocouple signal for the direct recording of $\chi(T)$.

Aging clearly causes a considerable increase in the ordering temperature, amounting to some 65°K after 1500 h. In addition, the critical peak becomes progressively broader, with an attendant reduction in its amplitude, although the area under the peak remains approximately constant. The apparent value of δ decreased with aging time (e.g., $\delta \approx 2.7$ after 387 h), as is to be expected from a spreading of the critical region.

Again, as in Fig. 4, the critical-peak positions always extrapolate to a zero-field T_c which coincides with the inflection point on the $\chi_0(T)$ curves. These curves are now more asymmetrical about T_c , with the inflection point occurring closer to the lower corner in $\chi_0(T)$; the region between T_c and the $\chi_0(T)$ maximum is very broad (~30°K) compared to that of the as-quenched sample (~5°K), suggesting a larger inhomogeneity in the ferromagnetic state of the sample after aging.

A rather extreme example of critical-peak broadening was shown by the cold-rolled sheet before it was heat treated; the critical peak, centered at $T_c \sim 210^\circ\text{K}$, was ~40°K wide, compared to ~10°K after quenching the sample (Fig. 2). The corresponding value of δ was ~2.2. Prior to measurement, this sample had been stored at room temperature for about one year, and thus 210°K is the practical upper limit of the ordering temperature of a cold-worked fully aged sample of the AuFe alloy composition studied here. It is doubtful, however, that significant aging effects occurred in this sample. The broadening is readily attributed to random strains in the sample.

As an aid in identifying the aging mechanism, we have plotted the as-quenched sample's order-

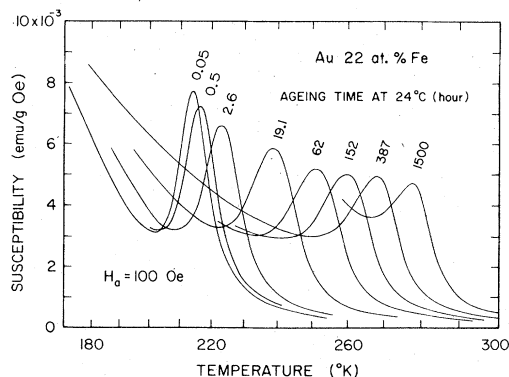


FIG. 6. ac susceptibility in the critical region, measured in an applied field of 100 Oe, as a function of room-temperature aging time.

ing temperature as a function of room temperature aging time t ; the most satisfactory relationship is the

$$\Delta T_c \propto \log_{10} t \quad (4)$$

dependence depicted in Fig. 7(a). There are some deviations from this behavior for the earliest aging times ($t < 0.5$ h), but there is some difficulty in selecting the true origin of the time scale, since aging effects occurring during the quench cannot be accounted for with any accuracy. Note, however, that the addition of about 1 h to the aging times allows all our data (extending over three decades of t) to be represented by Eq. (4).

A linear plot of $T_c(t)$ as shown in Fig. 7(b) indicates that on a laboratory time scale, the change in T_c reaches $\frac{2}{3}$ of its "saturated" value²⁵ in a time of about 60 h. We had hoped that accelerated aging of the sample at a higher temperature would produce a continuation of this behavior, but with a different characteristic time. It would then have been possible to estimate the activation energy of the aging process and, in turn, to identify its physical origin. Such an attempt was not successful with the sample which was preaged at 24°C. After only 15 min at 100°C, T_c was lowered from 277 to 260°K, instead of being raised. A further decrease to 255°K was found for times up to 3 h at 100°C, after which no measurable changes in T_c occurred. It seems obvious that, if an activation energy is to be deduced from the temperature of the rise in T_c caused by aging, the sample should always be used in the as-quenched state, for each aging temperature. This is especially true when we may not assume a linear dependence of T_c on the sample parameter directly affected by aging.

Figure 8 summarizes the changes in the critical peaks, in an applied field of 100 Oe, produced by the treatment at 100°C as well as at higher temperatures. The sample was exposed to these con-

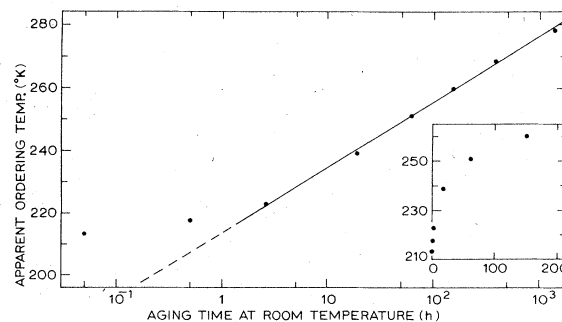


FIG. 7. Estimated ordering temperature T_c (°K) plotted against (a) the logarithm of the room-temperature aging time t (h). The inset (b) shows T_c plotted against t for laboratory times.

secutively increasing temperatures for around 15 h each, followed by a slow cooldown at 24°C, as determined by the cooling rate of the vacuum furnace. The high-temperature aging or annealing results in a continuous, rapid decrease in T_C , up to about 200°C, above which T_C changes more slowly towards an apparently final value of ~228°K. The positions of the critical peak at 100 Oe are plotted in Fig. 9.

The divergent behavior of T_C represented by Figs. 6 and 8 implies that either two distinct metallurgical processes are in operation over the temperature range investigated by us, or that the magnetic behavior reflects a single process in various stages of completion. We presently favor the latter interpretation, as will be discussed in Sec. V.

In addition to the reduction in T_C , the higher-temperature treatment produces a narrowing of the critical peak. The extent of this narrowing associated with "annealing" at 225°C surprisingly results in a peak even sharper than that of the sample originally quenched from 920°C as can be seen by comparing Figs. 6 and 8. The critical indices after the 225°C treatment, obtained from the plots in Figs. 3(b) and 5(b), are

$$\delta = 3.9 \pm 0.2 \text{ and } \gamma = 1.51 \pm 0.02.$$

The increased value of δ as well as the critical peak height are both consistent with a narrowing of the critical region, while this has no measurable effect on γ .

In the two cases where we have analyzed the critical behavior, we can extract values of the effective impurity moment μ_{eff} , for comparison with previous estimates and, more importantly, as a check on changes in this quantity, resulting from the presence of magnetic precipitates or

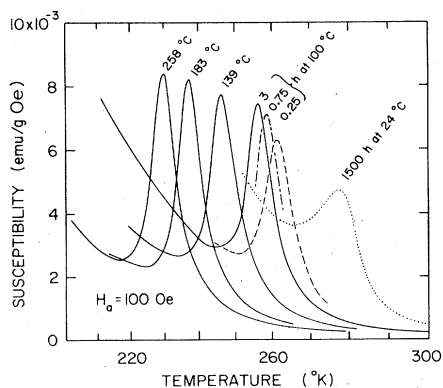


FIG. 8. ac susceptibility (in emu/g Oe) in the vicinity of the critical region, measured in an applied field of 100 Oe, after annealing at successively elevated temperatures (shown against the appropriate curve), subsequent to room-temperature aging.

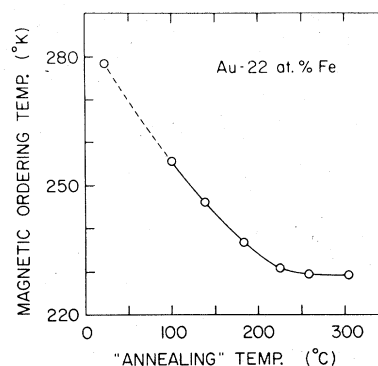


FIG. 9. Estimated magnetic-ordering temperature (°K), defined by the critical peak position in an applied field of 100 Oe (Fig. 8), as a function of (increased) annealing temperature (°C).

superparamagnetic clusters induced by the heat treatment.

The conventional manner of deducing μ_{eff} is from the observed Curie-Weiss behavior well above T_C . However, during the room-temperature aging experiment, no $\chi_0(T)$ data could be taken above 24°C, to avoid uncontrolled aging of the sample. For this reason we did not obtain values of γ and μ_{eff} for the long-aged samples, nor could we resort to a Curie-Weiss plot to find μ_{eff} for the sample even after the higher-temperature treatments, since T_C was always too close to these temperatures to obtain meaningful slopes. We therefore used the following approach; in the mean-field approximation (MFA),

$$\chi_0(T)^{\text{MFA}} = N\mu_{\text{eff}}^2 / 3k(T - \Theta) \quad (5)$$

in the usual notation. Within the MFA, $\Theta = T_C$

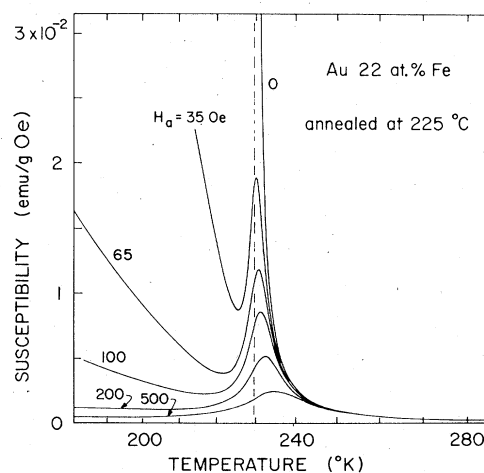


FIG. 10. ac susceptibility in the vicinity of the critical region in various dc applied fields, after annealing the sample for 15 h at 225°C. The dashed line locates the zero-field ordering temperature as defined by the inflexion point in $\chi_0(T)$.

and $\gamma=1$, so that we can write

$$\begin{aligned}\chi_0(T) &= \frac{N\mu_{\text{eff}}^2}{3k(T-T_C)} \left(\frac{T-T_C}{T_C} \right)^{1-\gamma} \\ &= \frac{N\mu_{\text{eff}}^2}{3kT_C} \left(\frac{T-T_C}{T_C} \right)^{-\gamma} = A^{\text{MFA}} e^{-\gamma}.\end{aligned}\quad (6)$$

Using series-expansion methods, Ritchie and Fisher²⁶ obtain

$$\chi_0(T) = A_c A^{\text{MFA}} \epsilon^{-\gamma}, \quad (7)$$

with $A_c \lesssim 1$ for the fcc structure with $S > 1$; A_c is slightly temperature dependent. Within the spirit of our approach we use

$$\chi_0(T) = A \epsilon^{-\gamma}, \quad \text{with } A = A^{\text{MFA}}. \quad (8)$$

Experimentally we find that $A = (2.95 \pm 0.2) \times 10^{-5}$ emu/g Oe for the as-quenched case ($T_C = 213.5^\circ\text{K}$) and $A = (2.53 \pm 0.2) \times 10^{-5}$ emu/g Oe following annealing at 225°C ($T_C = 229.5^\circ\text{K}$). The associated values of μ_{eff} are then $(6.2 \pm 0.2)\mu_B$ and $(6.0 \pm 0.2)\mu_B$, respectively, per Fe impurity atom. We take this constancy of μ_{eff} to be strong evidence against the presence of substantial clusters which are already magnetically ordered above T_C . Furthermore, despite the lack of extended $\chi_0(T)$ traces for the long-room-temperature-aged sample, a check at equivalent temperature increments above T_C shows no noticeable change in $\chi_0(T)$, suggesting overall constancy of μ_{eff} . The above value of μ_{eff} falls between previously reported results of Curie-Weiss analyses (e.g.,¹⁷ $4.7\mu_B$ and³ $10.5\mu_B$), which are higher than the value obtained from the saturation magnetization at low temperatures^{13,17} ($\mu_{\text{eff}} \sim 2.8\mu_B$), for Au-22-at.-%-Fe alloys.

We have no suitable explanation for the field dependence of the ordering temperature, seen in Fig. 4. The shift amounts to $\sim 10^\circ\text{K}/\text{kOe}$ in the low fields used here, and is almost independent of thermal history. Such a strong field dependence was not found in other alloys.^{18,19} By making the approximation $dT_C/dH = T_C/H_{\text{ex}}$, one obtains an effective exchange field $H_{\text{ex}} \approx 20\text{kOe}$; this may be compared with the effective field $H_{\text{ex}} = kT_C/\mu_{\text{eff}} \approx 500\text{kOe}$, using $\mu_{\text{eff}} \sim 6\mu_B$. However, we feel that this inconsistency should not be used as evidence of large-cluster behavior, because of the implied lack of variation in cluster size with heat treatment.

V. CONCLUSIONS

As we stated previously,¹⁸ and as the above results demonstrate, a greater insight into the magnetic-ordering process can be obtained by studying the critical behavior than by studying the reversal of the bulk magnetization associated with the prin-

cipal maximum in $\chi(T)$. The sharpness of the critical peak after the initial quench, as well as after annealing above room temperature, shows that we are dealing with a true long-range ferromagnet with little inhomogeneity. This should be contrasted with the condition of the sample after considerable room-temperature aging, which shows nonequilibrium conditions, resulting in a much broader critical peak. Whether this is due to microscopic phase separation into AuFe_3 and AuFe (as would be suggested by the Au-Fe phase diagram²⁷) we were unable to determine directly particularly in view of the subsequent behavior of the critical peak after higher-temperature treatment. Indirect evidence on this point is provided by the critical analysis which shows that the critical indices as well as μ_{eff} are not significantly affected by the sample treatment. In particular, this lack of variation in μ_{eff} argues against precipitation of $\alpha\text{-Fe}$ or AuFe_3 clusters during aging.

In this latter sense our work agrees with that of Borg and Dienes²⁸ who argue that the variation in magnetic properties of the AuFe system (at the concentration of interest here) is not caused by the nucleation and growth of a second phase but rather by the presence of short-range order induced by heat treatment through the change in proportions of like and unlike near neighbors relative to that of a random solid solution. Further, while we agree that the greatest sensitivity to short-range order in AuFe should occur near 17-at.-% Fe, where the magnetic order supposedly changes from mictomagnetic to long-range ferromagnetic, our samples showed marked thermal history effects even in the well-established ferromagnetic regime, contrary to previous results.²⁸

Variations in the rate of vacancy-aided diffusion and hence the degree of short-range order caused, for example,¹⁷ by the presence of local stresses, will lead to magnetic inhomogeneity within the sample after aging. This would account for the spreading of the critical peaks (Fig. 6) as well as the broadening and downward shift, relative to T_C , of the $\chi_0(T)$ maxima, since domain wall motion is expected to be the dominant process in the low-field magnetization reversal.

For AuFe alloys near the low-concentration end of the ferromagnetic regime and with a large number of quenched-in vacancies, we conclude that the initial rise in T_C induced by room-temperature aging is due to an increase in the number of magnetic nearest-neighbor interactions. It has been suggested⁸ that short-range order results in the interconnection of random chains of Fe atoms. We may postulate further that a continuation of this process, together with the annealing out of

vacancies at higher temperatures, produces a number of Fe sites with surroundings equivalent to fcc γ -Fe which will then have the effect of decreasing the number of ferromagnetic nearest-neighbor interactions, by analogy with CuFe .²⁹ It is thus implied that T_C will pass through a maximum during low temperature heat treatment. For higher temperatures or longer annealing times than were used in this work, any metastable γ -Fe regions will begin to precipitate as ferromagnetic bcc α -Fe,¹⁷ with very different magnetic consequences.

The low value of T_C in the cold-worked sample (slightly less than that of the rapidly quenched sample) and the apparent lack of aging effects is

consistent with the above explanation in that such a sample should represent a random solid solution. The low-equilibrium density of vacancies at room temperatures will greatly reduce the aging rate by inhibiting the short-range-ordering mechanism.

ACKNOWLEDGMENTS

It is a pleasure to thank Dr. P. Gaunt for the x-ray analyses and for several informative discussions and suggestions relating to the metallurgy of the AuFe system. This work has been supported in part by the National Research Council of Canada.

-
- *Present address: Eaton Electronics Research Lab., McGill Univ., Montreal, H3C 3G1, Canada.
- ¹A. P. Murani, S. Roth, P. Radhakrishna, B. D. Rainford, B. R. Coles, K. Ibel, G. Goeltz, and F. Mezei, *J. Phys. F* **6**, 425 (1976).
- ²D. E. Murnick, A. T. Fiory, and W. J. Kossler, *Phys. Rev. Lett.* **36**, 100 (1976).
- ³V. Cannella and J. A. Mydosh, *Phys. Rev. B* **6**, 4220 (1972).
- ⁴See, for example, J. A. Mydosh, P. J. Ford, M. P. Kawatra, and T. E. Whall, *Phys. Rev. B* **10**, 2845 (1974), and references therein.
- ⁵See, for example, L. E. Wenger and P. H. Keesom, *Phys. Rev. B* **11**, 3497 (1975), and references therein.
- ⁶C. E. Violet and R. J. Borg, *Phys. Rev.* **149**, 540 (1966).
- ⁷P. P. Craig and W. A. Steyert, *Phys. Rev. Lett.* **13**, 802 (1964).
- ⁸U. Gonser, R. W. Grant, C. J. Meechan, A. H. Muir, and H. Wiedersich, *J. Appl. Phys.* **36**, 2124 (1965).
- ⁹B. Window, *Phys. Rev. B* **6**, 2013 (1972).
- ¹⁰R. J. Borg and T. A. Kitchens, *J. Phys. Chem. Solids* **34**, 1323 (1973).
- ¹¹R. Tournier and Y. Ishikawa, *Phys. Lett.* **11**, 280 (1964).
- ¹²O. S. Lutes and J. L. Schmit, *Phys. Rev.* **134**, A676 (1964).
- ¹³J. Crangle and W. R. Scott, *J. Appl. Phys.* **36**, 921 (1965).
- ¹⁴B. de Mayo, *AIP Conf. Proc.* **5**, 492 (1972).
- ¹⁵R. J. Borg, D. Y. F. Lai, and C. E. Violet, *Phys. Rev. B* **5**, 1035 (1972).
- ¹⁶A. P. Murani, *J. Phys. F* **4**, 757 (1974).
- ¹⁷E. Scheil, H. Specht, and E. Wachtel, *Z. Metallk.* **49**, 590 (1958).
- ¹⁸I. Maartense and Gwyn Williams, *J. Phys. F* **6**, L121 (1976).
- ¹⁹I. Maartense and Gwyn Williams, *J. Phys. F* **6**, 2363 (1976).
- ²⁰R. M. Roshko and Gwyn Williams, *J. Low Temp. Phys.* **20**, 383 (1975).
- ²¹E. R. Jette, W. L. Bruner, and F. Foote, *Trans. AIMME* **III**, 354 (1934).
- ²²L. P. Kadanoff *et al.*, *Rev. Mod. Phys.* **39**, 395 (1967).
- ²³J. S. Kouvel and M. E. Fisher, *Phys. Rev.* **136**, A1626 (1964).
- ²⁴S. Arajs, B. L. Tehan, E. E. Anderson, and A. A. Stelmach, *Intern. J. Magnetism* **1**, 41 (1970).
- ²⁵In reality, of course, the T_C -vs- t curve should not saturate due to the $\log_{10} t$ dependence of T_C . However, this estimate suffices for our present purpose.
- ²⁶D. S. Ritchie and M. E. Fisher, *Phys. Rev. B* **5**, 2668 (1972).
- ²⁷M. Hansen and P. Anderko, *Constitution of Binary Alloys* (McGraw-Hill, New York, 1958), p. 204.
- ²⁸R. J. Borg and G. J. Dienes, *J. Appl. Phys.* **46**, 99 (1975).
- ²⁹B. Window, *Philos. Mag.* **26**, 681 (1972).